Plant Nano Biology 9 (2024) 100091

Contents lists available at ScienceDirect

Plant Nano Biology

journal homepage: www.journals.elsevier.com/plant-nano-biology

Sustainable crop fertilization by combining biogenic nano-hydroxyapatite and P solubilizing bacteria: Observations on barley

Laura Pilotto [a,b], Monica Yorlady Alzate Zuluaga [d], Francesca Scalera [c], Clara Piccirillo [c], Luca Marchiol [a,*], Marcello Civilini [a], Youry Pii [d], Stefano Cesco [d], Guido Fellet [a]

[a] Department of Agrifood, Environmental and Animal Sciences, University of Udine, Udine, Italy
[b] Department of Life Sciences, University of Trieste, Trieste, Italy
[c] Institute of Nanotechnology CNR-NANOTEC, Lecce, Monteroni, Italy
[d] Faculty of Science and Technology, Free University of Bozen/Bolzano, Bolzano, Italy

ARTICLE INFO

Keywords:
Food Industry residues
Hordeum vulgare
Nanofertilizers
NHAP
Pseudomonas alloputida

ABSTRACT

Nano-enabled agriculture involves researching smart nano-agrochemicals for sustainable farming. Nano-hydroxyapatite (nHAP), a phosphorus-rich compound, has the potential to be used as a fertilizer with reduced environmental impact. This study tests the effectiveness of nHAP produced from waste materials (animal bones) on barley plants (*Hordeum vulgare*). Two different nHAPs were prepared by thermal treatment of chicken bones at 300 °C and 700 °C ($nHAP_{300}$ and $nHAP_{700}$, respectively). The nanopowders were then tested in a seed toxicity trial and in a greenhouse pot experiment with barley, using *Pseudomonas alloputida*, a P-solubilizing bacterium (PSB). The treatments were unfertilized soil, conventional triple superphosphate (TSP), and the nHAP treatments alone. The results indicated that: (i) the nHAP materials had particle sizes of 1 micrometer ($nHAP_{300}$, due to aggregation) and 50–70 nm ($nHAP_{700}$), with P contents of 12.8 % and 19.6 %, respectively; (ii) no toxicity was observed on barley seeds, and $nHAP_{300}$ at maximum dose stimulated root length by 45.6 % compared to the control; (iii) compared to conventional P fertilizer TSP, $nHAP_{300}$ and $nHAP_{700}$ stimulated root growth by 7 % and 18 %, respectively; (iv) the fraction of available P produced through $nHAP_{300}$-PSB (40.6 mg kg^{-1}) was higher than that from TSP (39.2 mg kg^{-1}); (v) ions associated with the nHAP structure supplied supplementary nutrients, predominantly allocated in root tissues. This study provides valuable insights for future investigations to assess the implications of P nano-fertilizations in achieving sustainability in agriculture.

1. Introduction

Nanotechnology holds promise in providing crucial tools to support the transition towards a sustainable agriculture model. Nano-enabled agriculture involves the application of engineered nanomaterials (ENMs) in agriculture (Kah et al., 2019; Lowry et al., 2019). The unique properties of ENMs, such as smaller size and larger surface area compared to bulk materials, are expected to facilitate the design of more efficient nano-agrochemicals with slower active ingredient release, prolonged retention of active compounds on plant leaves, and enhanced effectiveness at lower doses (Singh et al., 2021; Xin et al., 2020).

The challenge of phosphorus fertilization in crop production is one of the key hurdles to overcome in achieving sustainable primary production. Typically, only around 20–25 % of the total amount of phosphate fertilizers applied is utilized by crops (Yu et al., 2021). This inefficiency necessitates a much higher supply of phosphorus to meet crop demands, leading to adverse effects on soil properties, freshwater quality, and eutrophication (Tiecher et al., 2023). Moreover, phosphorous is often already present in agricultural soils in high concentrations, but it is not bioavailable.

Soil microorganisms play a crucial role in the soil-plant phosphorus cycle. Specifically, specialized phosphate-solubilizing bacteria (PSB) can convert immobilized phosphorus into mineral forms, and organic residues into available phosphorus for plant uptake. However, the current understanding of how PSB (phosphate-solubilizing bacteria) work in fertilizing crops and how they are used in the field is incomplete. While it's unlikely that PSB alone can meet all of a crop's nutrient needs, it is realistic to hypothesize that in the future they may be combined with nanomaterials to improve their ability to colonize plants and extend their shelf life. This underscores the urgent need for further research in

* Corresponding author.
E-mail address: luca.marchiol@uniud.it (L. Marchiol).

https://doi.org/10.1016/j.plana.2024.100091
Received 20 June 2024; Received in revised form 31 July 2024; Accepted 4 September 2024
Available online 12 September 2024

this area (Cheng et al., 2023).

Hydroxyapatite (HAP), a calcium phosphate compound, with a stoichiometric formula of $Ca_{10}(PO_4)_6(OH)_2$ and a Ca/P molar ratio of 1.67, is a major inorganic component of animal bones and teeth (Maschmeyer et al., 2020). It was extensively investigated in biomedical and industrial applications. Recently, nanoscale-sized HAP (nHAP) garnered attention for its potential application as a fertilizer. Leveraging its high surface-to-volume ratio, characteristic of nanoscale materials, nHAP could be utilized for surface impregnation and functionalization with fertilizers and macronutrient molecules, thus enabling the development of advanced nanohybrids in agriculture (Maghsoodi et al., 2020; Fellet et al., 2021; Carmona et al., 2022).

The traditional production methods of engineered nanomaterials using chemical and physical processes often use toxic and flammable chemicals, resulting in expensive production and the generation of hazardous by-products (Baig et al., 2021). Consequently, a significant effort was made to investigate alternative methods such as biosynthesis. By the principles of green chemistry, this approach makes it possible to produce nanomaterials at room temperature and pressure with a more limited impact on the environment.

Several methods exist for producing nHAP powder via chemosynthesis (Dou et al., 2018). The literature contains numerous studies exploring the potential use of synthetic nHAP in agriculture. The first study investigating the fertilizing potential of nHAP was carried out in greenhouse conditions on *Glycine max* by (Liu et al., 2015).

Fellet et al., (2021) reviewed the research development on the use of nHAP for plant nutrition, identifying three main directions: (i) the use of nHAP for phosphate nutrition, (ii) the synthesis of hybrid nanostructures consisting of nHAP associated with urea, and (iii) the use of nHAP as a carrier for micronutrients. The studies were conducted on widely spread cultivated herbaceous species such as *Triticum aestivum* (Montalvo et al., 2015), *Helianthus annuus* (Xiong et al., 2018), *Zea mays* (Yoon et al., 2020; Gunes et al., 2024), *Oryza sativa* (Madusanka et al., 2017; Kottegoda et al., 2017; Pradhan et al., 2021), *Hordeum vulgare* (Szameitat et al., 2021) and *Solanum lycopersicum* (Marchiol et al., 2019), and also on *Camellia sinensis* (Raguraj et al., 2020), *Lactuca sativa* (Sakhno et al., 2022), *Vigna radiata* (Subbaiya et al., 2012) and *Asparagus officinalis* (Phan et al., 2019) and the forage species *Festuca arundinacea* (Gunaratne et al., 2016).

The biosynthesis of nHAP was studied by Priyam et al., (2019), who developed an environment-friendly synthesis route mediated by the solubilization of P by organic acids extracellularly secreted by *Bacillus licheniformis*. This biogenic nHAP was positively tested on plants in two experiments. nHAP was supplied via fertigation to *Oryza sativa* subsp. *japonica* cultivated in low- and high-calcareous soil (Priyam et al., 2022a) and tested as fertilizer on *Solanum lycopersicum* L. grown in soils with different pH (Priyam et al., 2022b).

Recently, researchers have started studying the use of biowastes to produce biogenic nHAP. This method provides a sustainable way to manage residues from the food industry, reducing the strain on landfills and decreasing the need for incineration. By-products from animal livestock and fishing, such as animal bones and fish bones, heads, skins, and scales, contain HAP as a main component that can be extracted (Piccirillo et al., 2017; Alao et al., 2017). The extraction process usually involves thermal treatments to reduce or eliminate organic components in the biowastes, followed by mechanical processes to reduce the powder to a nanometric scale, resulting in nHAP (C. Teixeira et al., 2017). Unlike the synthetic form, biogenic nHAP contains magnesium, sodium, carbonate ions, and various trace elements such as potassium, fluoride, chloride, and zinc ions (Cestari et al., 2021); these ions could be beneficial for some applications including agriculture, as they could have an impact on plants growth.

Ahmed et al. (2021) conducted a methodological study on the thermal treatment conditions used to extract biogenic nHAP. Analysis of the chemical composition and of the calcium phosphate phases present (performed with X-ray diffraction (XRD) and Fourier transform infra-red spectroscopy (FTIR) were used to elucidate P solubility and bioavailability in nHAP obtained from different thermal processing methods (pyrolysis vs. combustion), heating temperatures (300 °C, 500 °C, 700 °C and 900 °C), and various animal bones (sheep, pigs and chicken). The fertilizing effects of the nHAPs were tested in a pot experiment growing *Lactuca sativa* for eight weeks on two soils with low and high pH, respectively. The most important result was that processing bones below temperatures of 700 °C resulted in higher P solubility. Chicken bone showed the highest water-soluble P content, irrespective of processing methods and temperatures. Furthermore, the P-fertilizing value of nHAPs was more pronounced in soil with a lower pH (Ahmed et al., 2021). A second study dedicated to the development of the biogenic nHAP synthesis procedure was conducted by Pohshna and Mailapalli (2023). In this case, the study concerned the grinding parameters of the starting material - in this case, eggshells - performed with a planetary ball mill. Considering that the technical variables of the milling process (speed, milling time, ball-to-powder ratio, milling medium and process temperature) certainly influence the size and shape of nHAP, it is evident that these parameters must be optimized. However, eggshells do not contain P, and this had to be added, reducing the sustainable aspect of this process. Biogenic nHAP of 105 nm was obtained from the preparation. Administered to *Oryza sativa* in field column experiments, it allowed a significant reduction in P leaching and an increase in grain yield compared to conventional P fertilization (Pohshna and Mailapalli, 2023).

According to current research, the use of nano-hydroxyapatite (nHAP) in phosphate fertilization is of particular interest due to its ability to release phosphorus slowly and enhance phosphate mobility compared to traditional P fertilizers (Xiong et al., 2018). However, there is a need to explore further the impact of nHAP on the microbial components of the soil-plant system. The effects of nHAP on plant-associated microbial communities are not yet fully understood. Nevertheless, studies are underway to examine the relationship between nHAP and phosphate-solubilizing bacteria (PSBs). This is important because PSBs play a role in the P release process in soil by nHAP. Therefore, gaining a better understanding of the dynamics of this process could be valuable for improving the modulation of P release from nHAP (A. Santana et al., 2019; Monroy Miguel et al., 2020; Jia et al., 2022).

This study aimed to evaluate the effectiveness of two types of biogenic nHAP, produced from chicken bones under different thermal treatment conditions, in serving as a phosphorus source for barley (*Hordeum vulgare* L.). The nHAP and the phosphate-solubilizing bacteria *Pseudomonas alloputida* KT2440 were combined and administered to the plants. The experiment focused on barley, the fourth most widely cultivated cereal worldwide. Cultivated in highly productive agricultural systems and marginal and subsistence environments, this crop is also significant economically for animal feed and alcohol production.

2. Materials and methods

2.1. nHAP synthesis and characterization

Nano-hydroxyapatite (nHAP) was obtained through the “top-down” procedure. Waste chicken bones were selected as the initial material for preparing nHAP. In the initial phase, the bones underwent heating at 80 °C in distilled water for 1 hour, followed by thorough washing to eliminate any residues. The bones were then subjected to calcination at either 300 °C (resulting in $nHAP_{300}$) or 700 °C (resulting in $nHAP_{700}$), employing a temperature ramp of 5 °C/minute and a dwell time of 1 hour. The obtained materials were finally mechanically milled to reduce and standardize their size (40 and 10 minutes, respectively for $nHAP_{300}$, and $nHAP_{700}$), at 40 Hz using a ball mill (MM2 Mixer Mill, Retsch, Düsseldorf, Germany) equipped with zirconia jars and balls.

The morphology of biowaste materials was analyzed by scanning electron microscopy (SEM) using a Carl Zeiss Merlin instrument, equipped with a Gemini II column and an integrated high-efficiency In-

lens for secondary electrons. Samples were sputtered with gold before the analysis. The phase composition of the nanopowders was determined by X-ray diffraction (XRD) with an X' Pert PRO MRD diffractometer, equipped with a fast RTMS detector, using a CuKα radiation (40 kV and 40 mA). Data were recorded in the 20–60° 2θ range, with a virtual step-scan of 0.02°, and virtual time-per-step of 200 seconds.

To determine their elemental composition, powders were then mineralized following the U.S. EPA 3052 protocol (US EPA, 1996a) with some modifications. Samples were digested in a microwave oven (Milestone Ethos Easy, Sorisole (BG), Italy) in Teflon vessels with 9 mL of HNO_3 and 1 mL of H_2O_2, and subsequently analyzed using inductively coupled plasma optical emission spectroscopy (ICP-OES) to determine the elemental content (Agilent 5800, Santa Clara, CA, USA).

2.2. Toxicity evaluation during the seed germination

A germination trial was conducted following the U.S. EPA OPPTS 850.4200 protocol (US EPA, 1996b) with modifications. Briefly, barley seeds (*Hordeum vulgare* L., cv. Marjory, SIS Società Italiana Sementi, San Lazzaro di Savena, Italy) were rinsed in Milli-Q water (Millipore Sigma Merck KGaA, Darmstadt, Germany) three times and then left to dry. Floating seeds were discarded. Five levels of $nHAP_{300}$ and $nHAP_{700}$ suspensions were tested: (i) 0 ppm, (ii) 10 ppm, (iii) 100 ppm, (iv) 1000 ppm and (v) 10,000 ppm. nHAP suspensions were prepared using Milli-Q water and sonicated for 30 minutes. Then, seeds were transferred to flasks with 40 mL of the different suspensions. Flasks were placed in a magnetic stirrer for 8 h to allow seeds imbibition.

Twenty seeds for each replicate were transferred to Petri dishes with filter paper soaked with Milli-Q. Five replicates per treatment were set up. Petri dishes were placed in a growth chamber in dark conditions at 25.0 ± 0.5 °C (FA-GO1400, Frigomeccanica Andreaus, Padova, Italy). After 3 days, the number of germinated seeds rate per plate and roots elongation were measured.

2.3. Pot experiment

2.3.1. Bacterial inoculant

Pseudomonas alloputida KT2440 strain DSM 6125 (DSMZ, Leibniz Institute, Braunschweig, Germany) was chosen based on its ability to solubilize tricalcium phosphate (TCP, $Ca_3(PO_4)_2$). The bacterial strain was grown in Luria–Bertani (LB) medium under orbital shaking at 180 rpm, 28 °C for 48 hours. Cells were then collected by centrifugation at 5000 x g for 10 minutes, washed, and re-suspended in a sterile saline solution (0.85 % w/v NaCl). The bacterial suspension was then adjusted to 10^8 cells mL^{-1} and was used as an inoculant, as described in the experiment below.

2.3.2. Plants growth

A sandy loam soil (pH, 7.6; sand 56 %, silt 30 % and clay 14 %; organic matter content, 4.4 %; cation exchange capacity, 13.9 cmol kg^{-1} DM; electrical conductivity, 434 µS m^{-1}, P-bioavailable (Olsen method) 38.8 mg kg^{-1}) was used in a pot experiment carried out in a semi-sealed greenhouse under full sunlight at the "A. Servadei" Experimental Farm of the University of Udine (Udine, Italy 46° 04' 52'' N, 13° 12' 33'' E). The soil was air-dried at room temperature and sieved through a 1 cm mesh. Five-liter pots were loaded with 2.6 kg of soil. Basal N-K fertilization was provided at the rate of 100 kg ha^{-1} and 83 kg ha^{-1} as $Ca(NO_3)_2$ and KNO_3, respectively. The P treatments included: unfertilized soil, conventional triple superphosphate (TSP), $nHAP_{300}$ and $nHAP_{700}$. The equivalent of 80 kg ha^{-1} of P was applied for each treatment (approximately 0.30–0.60 g of fertilizer, based on the P content of the fertilizer). All NPK fertilizers were mixed with soil during the pot-filling procedure. To investigate the potential of enhancing the P-bioavailability for nanoparticles and facilitate the P-uptake, the same treatments were repeated with the inoculum of a *P. alloputida* (PSB) suspension. The final treatments were: unfertilized soil (Ctrl), (ii) Ctrl+PSB, (iii) TSP, (iv) TSP+PSB, (v) $nHAP_{300}$, (vi) $nHAP_{300}$+PSB, (vii) $nHAP_{700}$, (viii) $nHAP_{700}$+PSB. Each treatment was replicated five times. Ten barley seeds (*Hordeum vulgare* L., cv. Marjory, SIS Società Italiana Sementi, San Lazzaro di Savena, Italy) were planted 1 cm deep in each pot. One week after the germination, seedlings were thinned down to 1 per pot. The bacteria inoculant (2 mL per plant, paragraph 2.3.1) was provided twice, the first time at the 3rd-true-leaf stage and the second one 35 days later. The same amount of sterile saline solution was used for treatments (i), (iii), (v), and (vii). During the growth period, the pots were individually weighed and irrigated with tap water to maintain the soil at 60 % of water holding capacity (WHC). Plants were harvested at the end of the tillering phase. Fresh plant biomass was separated into roots and shoots and fresh weights were recorded. Plant fractions were oven-dried at 72 °C for 48 hours and weighed. Ionomic analyses were then conducted. For these analyses, Millipore-Sigma products (Merck KGaA, Darmstadt, Germany) were used without any further purification. Dried root and shoot samples were digested following the EPA 3052 (US EPA, 1996a) and analyzed by ICP-OES. Elements detected were P, K, Ca, Mg, S, Fe and Mn. At the end of the experiment, soil samples were collected as well to determine P-bioavailability. The Olsen methodology was applied, with some modifications. 2 g of air-dried soil and 40 mL of extractant solution ($NaHCO_3$ 0.5 M, pH =8.5) were shaken for 30 minutes. The supernatant was then filtered and analyzed by ICP-OES.

2.4. Data analysis

The germination test data were analyzed using R (version 4.2.1) and R Studio (version: 2023.09.1+494) to calculate mean values and standard errors. Subsequently, a one-way ANOVA and post-hoc Tukey test ($p \leq 0.05$) were performed. Germination percentage was determined using Eq. (1):

$$\%Germination = \frac{Number\ of\ seeds\ germinated}{Total\ number\ of\ seeds} \times 100 \quad (1)$$

Seedlings were photographed, and Image J software (version: 1.54 h) was utilized to measure root lengths. Root elongation was recorded for each root per seed, and the average was computed using Eq. (2):

$$Mean\ root\ length = \frac{\sum length\ of\ each\ root\ per\ seed}{number\ of\ roots\ per\ seed} \quad (2)$$

The greenhouse trial followed a completely randomized experimental design with two main factors: (i) type of P fertilizer (FERT) and (ii) presence or absence of the P-solubilizing bacteria (PSB) *Pseudomonas alloputida*. Factor FERT comprised four levels: Ctrl, TSP, $nHAP_{300}$, and $nHAP_{700}$, each replicated five times. Grubbs' Test was employed to identify outliers and certain data points were excluded before conducting the one-factor and two-ways ANOVA ($p \leq 0.05$). Data were transformed as necessary to ensure variance homogeneity and approximate normal distributions. Tukey's Multiple Comparison test ($p = 0.05$) was utilized to evaluate individual effects in cases of significant results. Different letters in tables and figures denote statistically significant differences in means. Stars indicate statistical significance: $p < 0.05$ was marked with one star (*), $p < 0.01$ was marked with two stars (**), and $p < 0.001$ was marked with three stars (***).

3. Results

3.1. Characterization of HAP_{300} and HAP_{700}

The surface morphology of $nHAP_{300}$ and $nHAP_{700}$ derived from chicken bones was examined using SEM. Fig. 1(a) and (b) depict SEM micrographs illustrating the distinct characteristics of the two nanopowders. $nHAP_{300}$ powders exhibit significant agglomeration, with nanometric-sized particles aggregating into larger ones exceeding 1 µm

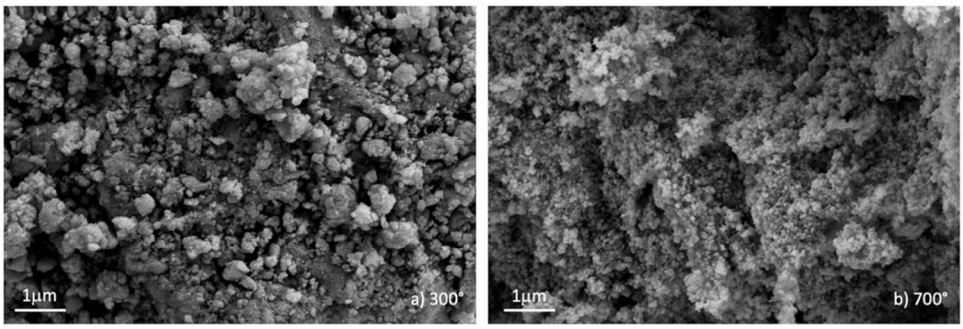

Fig. 1. SEM images of a) $nHAP_{300}$ and b) $nHAP_{700}$ at 30k magnification.

in size.

These particles have an almost regular spherical shape, with micron-sized pores observed between them. Conversely, $nHAP_{700}$ nanopowders display smaller dimensions, approximately 50–70 nm, with a more regular size distribution and no apparent agglomeration. This difference could be attributed to the higher temperatures employed during the deproteinization process, facilitating the removal of organic matter, and resulting in particle disaggregation.

XRD patterns of $nHAP_{300}$ and $nHAP_{700}$ powders are presented in Fig. 2. $nHAP_{300}$ analysis reveals very broad diffraction peaks, indicative of low crystallinity, due the low-temperature treatment, with the main peak at 31.7° corresponding to hydroxyapatite (Scalera et al., 2013). As the calcination temperature increases from 300 °C to 700 °C, peak intensity enhances and peaks become narrower, suggesting the removal of proteins and organics, as well as crystal coalescence and growth (Scalera et al., 2013). The crystalline composition of $nHAP_{700}$ closely aligns with hydroxyapatite, corroborated by comparison with the Joint Committee on Powder Diffraction Standards (JCPDS 09–0432) data. Additionally, secondary phases such as β-tricalcium phosphate (β-TCP) (JCPDS NO9–169) are detected in $nHAP_{700}$ (Gervaso et al., 2012), indicated by asterisks in the figure.

Elemental analysis of both powders reveals a Ca/P molar ratio lower than the stoichiometric value of 1.67—specifically 1.50 for $nHAP_{300}$ and 1.47 for $nHAP_{700}$. These values explain the formation of β-TCP in $nHAP_{700}$, as its stoichiometric ratio aligns closely with that of the powder. Indeed, the thermal treatment initiates a partial conversion of hydroxyapatite to β-TCP, resulting in biphasic calcium phosphate (BCP) formation, as evidenced by XRD data.

Table 1 presents elemental analysis results, indicating a higher concentration of C (31.3 %) and N (5.6 %) in $nHAP_{300}$, likely due to incomplete combustion of organic matter. Conversely, these elements are only present in low concentrations (< 1 %) in $nHAP_{700}$, suggesting near-complete combustion. Consequently, other elements (e.g., K, Mg, Mn) exhibit higher concentrations in $nHAP_{700}$.

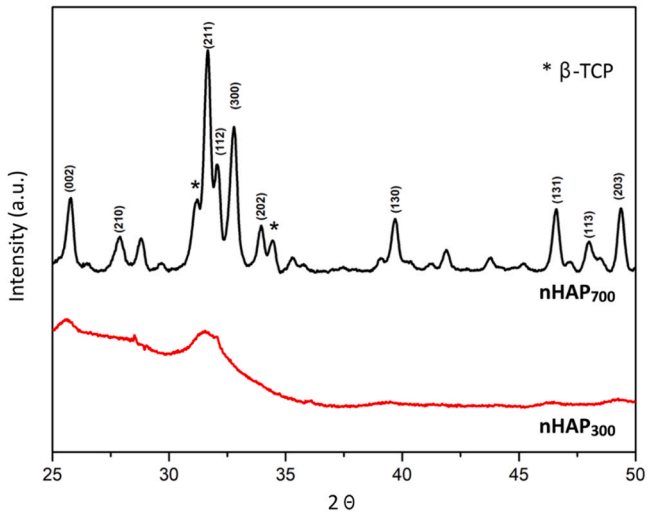

Fig. 2. XRD patterns for $nHAP_{300}$ and $nHAP_{700}$ powders.

Table 1
Concentration of elements present in the structure of $nHAP_{300}$ and $nHAP_{700}$.

Element		$nHAP_{300}$	$nHAP_{700}$
C	(%)	31.3 ± 0.28	0.4 ± 0.026
Ca	(mg kg^{-1})	246 ± 5.84	373 ± 5.78
Cu	(mg kg^{-1})	0.27 ± 0.47	1.34 ± 1.53
Fe	(g kg^{-1})	0.16 ± 0.01	0.23 ± 0.02
K	(g kg^{-1})	0.66 ± 0.05	1.19 ± 0.02
Mg	(g kg^{-1})	5.45 ± 0.03	8.07 ± 0.04
Mn	(mg kg^{-1})	4.41 ± 0.04	6.95 ± 0.07
N	(%)	5.58 ± 0.151	0.06 ± 0.01
P	(g kg^{-1})	128 ± 2.77	196 ± 2.31
S	(g kg^{-1})	1.24 ±0.11	2.30 ±0.25

3.2. Seed germination

The barley kernels were at a developmental stage between radicle emergence and coleoptile emergence, at the time of measurement. Although there was significant variability, it was still possible to identify seeds with primary roots, seminal roots and, in many cases, a young coleoptile (Fig. 3).

The percentage of germination and the seed average root length observed in *H. vulgare* are reported in Fig. 4.

The statistical analysis indicated that nHAP did not affect the germination of *H. vulgare*. The average germination rate across all treatments was 77 % (291 out of 380 seeds), as shown in Fig. 4 A. The number of roots formed by each germinated seed, including the primary root axis and secondary roots, was recorded. The treatments did not have a statistically significant effect on root formation; the average number of roots per seed was 5.60 and 5.52 for $nHAP_{300}$ and $nHAP_{700}$, respectively. In contrast, root growth, represented by the average root length per seed, responded to the treatments. In particular, the ANOVA revealed a significant effect of treatments with $nHAP_{300}$ ($F(4,20) = 3.3320$, $p = 0.0303$ *), promoting a progressive increase in root development. Compared to the control, the root length of *H. vulgare* seedlings increased by 23 % (100 ppm) and 45.6 % (10,000 ppm), respectively (Fig. 4B). The same evidence was observed for nHAP700 ($F(4,20) = 4.9659$, $p = 0.0060$ **). In this case, and at the same concentrations, the increase in root development was 43.5 % and 31.4 % (Fig. 4 C). A specific variability in the data disturbed the linear progression, which is less clear than that with $nHAP_{300}$; however, with $nHAP_{700}$ the increase in root development occurs at lower concentrations.

3.3. Plant growth

The experimental data underwent two-way ANOVA analysis to

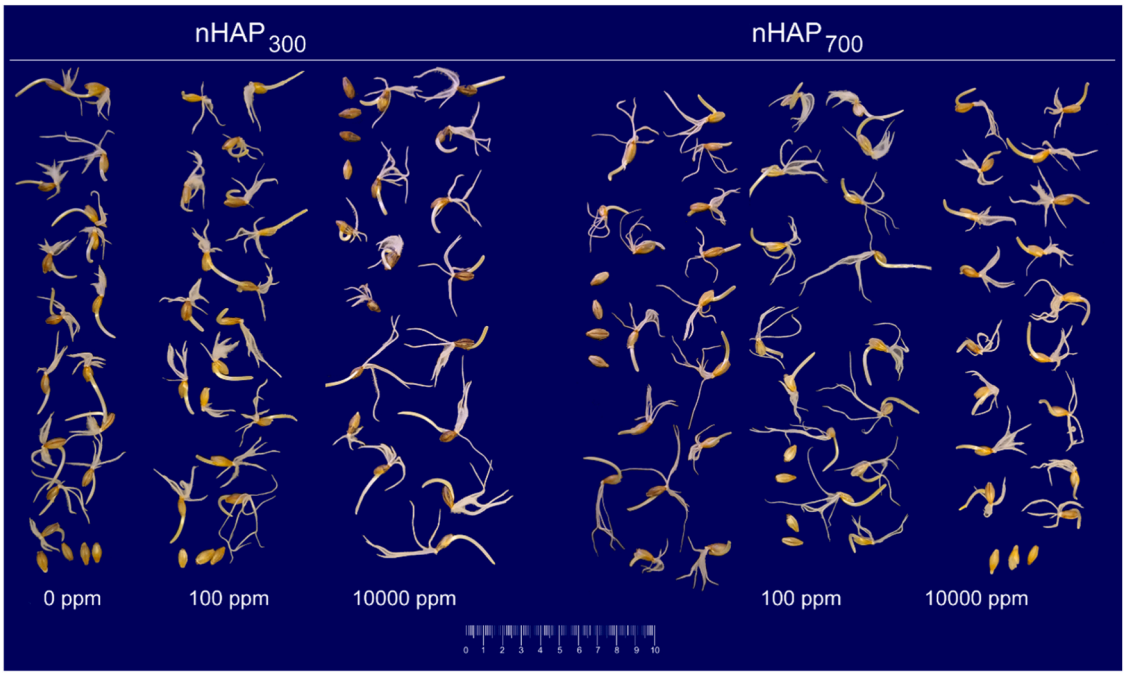

Fig. 3. Germinated seeds of *H. vulgare* pre-treated with $nHAP_{300}$ and $nHAP_{700}$ 0–10000 ppm.

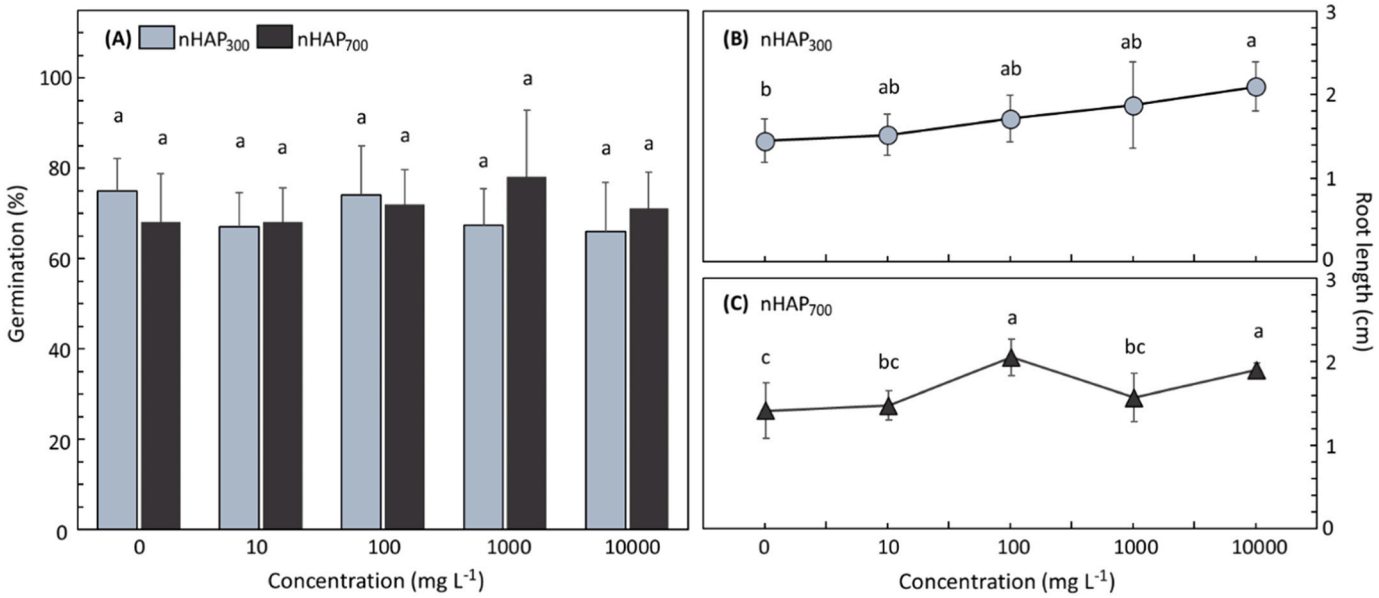

Fig. 4. (A) Germination percentage in seeds of *H. vulgare* exposed to different concentrations of $nHAP_{300}$ and $nHAP_{700}$. (B-C) Average root length (cm) in barley seedlings. Data are mean ± standard error (n=5). Different letters were used to indicate statistically significant differences between treatments with Tukey's post-hoc test ($p \leq 0.05$).

detect the interaction between the experimental factors FERT and PSB. The initial findings focused on biometric variables. It was observed that the interaction between PSB and FERT did not significantly affect the dry weight of the roots ($F(7,32) = 0.9258$, $p = 0.4395$). As regards the main effects, the FERT factor had a significant impact on the dry matter of the barley plant roots ($F(7,32) = 5.5858$, $p = 0.0034$ **), whereas PSB factor did not ($F(7,32) = 0.1934$, $p = 0.1215$). As expected, P-fertilized plants showed more root biomass than the control group. Interestingly, the plants that received $nHAP_{300}$ and $nHAP_{700}$ developed even higher root biomass compared to those fertilized with TSP (Fig. 5).

The difference between the $nHAP_{300}$ (6.37 g plant^{-1}), $nHAP_{700}$ (7.46 g plant^{-1}) and TSP treatment (6.20 g plant^{-1}) is significant at the post-hoc Tukey test, based on quantitative comparisons. Fertilization with $nHAP_{300}$ and $nHAP_{700}$ increased root biomass production by 7 % and 18 %, respectively, compared to TSP (Fig. 5).

It was observed that the treatments had no impact on the development of aerial biomass (data not shown). Therefore, it was expected that the total weight of the barley plants would confirm the same for the root biomass, which was found to be true, as shown in Fig. 6.

Additionally, there was no significant interaction between FERT and PSB on the total plant biomass, as confirmed by the statistical analysis ($F(7,32) = 0.4680$, $p = 0.7067$). However, the application of FERT resulted in a positive response from the barley plants ($F(7,32) = 3.3658$, $p = 0.0305$*), while the contribution of PSB on plant growth was

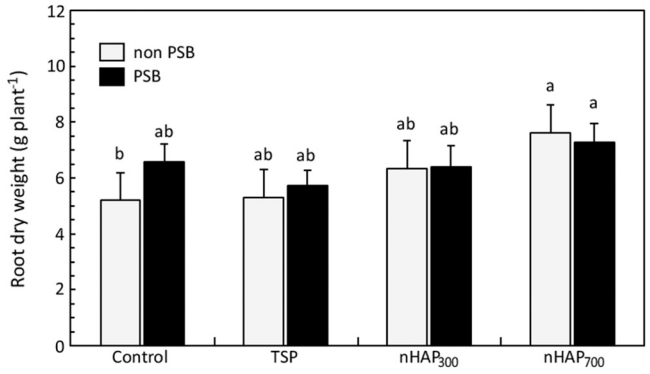

Fig. 5. Root dry weight observed in plants of *H. vulgare* grown in unfertilized soil (Control), or treated with TSP, nHAP$_{300}$, and nHAP$_{700}$. In addition, soils were either not inoculated (non PSB) or inoculated with *P. alloputida* (PSB). Bars are standard deviation (n = 5). Letters indicate statistically significant differences between treatments with Tukey's Multiple Comparison test (p=0.05).

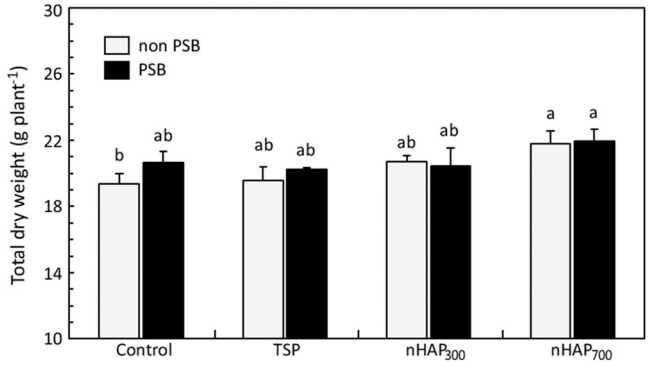

Fig. 6. Total dry weight observed in plants of *H. vulgare* grown in unfertilized soil (Control), or treated with TSP, nHAP$_{300}$, and nHAP$_{700}$. In addition, soils were either not inoculated (non PSB) or inoculated with *P. alloputida* (PSB). Bars are standard deviation (n = 5). Letters indicate statistically significant differences between treatments with Tukey's Multiple Comparison test (p=0.05).

negligible (F(7,32) = 0.8146, p=0.3738).

After registering that the plants did not respond to the PSB treatment, the average plant total dry weight (n=10) was calculated for the FERT treatment. The post-hoc test for the main factor FERT showed a significant difference between the means. The total dry weight of the plants showed an increase of 3.42 % and 10 % for nHAP$_{300}$ and nHAP$_{700}$ treatments, respectively, compared to TSP (Fig. 6).

3.4. Soil available P

The soil available P was evaluated using the Olsen method. As for the biometric data, we employed a two-factor ANOVA for an overall view of the data and possibly highlighted the FERT x PSB interaction. The interaction was not significant, while the effect of the PSB factor on Olsen P was highly significant. In the average fertilizer treatments, the post-hoc Tuckey's test indicated 38.7 mg P kg^{-1} and 35.8 mg P kg^{-1}, respectively, for PSB and non PSB.

In Fig. 7, the data of available P associated with the results of the Tukey test are reported (p=0.05). More exactly, the significant effect of the PSB factor was verified by conducting a pairwise t-test between PSB/non PSB Ctrl soil (p=0.034*) and PSB/non PSB nHAP$_{300}$ soil (p=0.0011**).

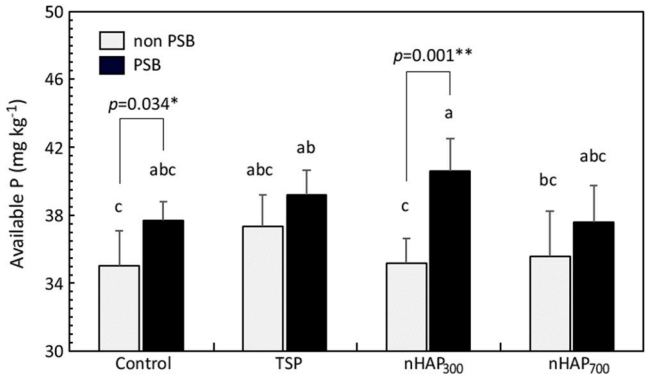

Fig. 7. Available P (mg kg^{-1}) detected in Ctrl, Ctrl+PSB, TSP, TSP+PSB, nHAP$_{300}$, nHAP$_{300}$+PSB, nHAP$_{700}$ and nHAP$_{700}$+PSB soils at the end of the experiment. Bars are standard errors (n = 5). Letters indicate statistically significant differences between treatments with Tukey's Multiple Comparison test (p=0.05). *p* refers to the pairwise t-test.

3.5. Elements in plant fractions

The first element of interest was the P supplied to the plants through TSP and nHAP. Regarding P levels in root tissues (Table 2) the two-factors ANOVA did not reveal any statistically significant effects of the main factors. The fertilizing treatments did not affect the root P allocation (p = 0.0872), and the presence of PSB did not show any significant impact, either (p = 0.1234). However, a statistically significant interaction effect (F(7,32) = 3.1939, p = 0.0366*) between the type of P fertilization and the presence or absence of PSB was observed. Quantitatively, the concentration of P in the plant roots ranged from 863 to 993 mg kg^{-1}. Combining P concentration data and the root dry weight, the amount of P allocated in plant roots was calculated (mg P plant^{-1}). As expected, FERT significantly influenced the root P content (F(7,32) = 3.3121, p = 0.0091**), which ranged between 5.15 and 7.06 (mg P plant^{-1}) for Ctrl and nHAP$_{700}$-PSB plants, respectively (Table 2).

Regarding the aerial biomass of barley, on the other hand, there was a significant effect of the PSB factor (F(1,32) = 7.0598, p = 0.0122*) on the concentration of P in the leaves and stems; however, there was no significant interaction of FERT x PSB. On average, the concentration of P was found to be 1055 and 1010 mg kg^{-1} in the PSB and non-PSB plants,

Table 2
Root and shoot P concentration (mg kg^{-1}), root and shoot P content (mg plant^{-1}) in plants of *H. vulgare*. Data are mean ± standard error (n=5). Different letters were used to indicate statistically significant differences between treatments with Tukey's post-hoc test (p ≤ 0.05).

Treatment	Root P concentration (mg kg^{-1})	Root P content (mg plant^{-1})	Shoot P concentration (mg kg^{-1})	Shoot P content (mg plant^{-1})
Ctrl	993 ± 50 a	5.16 ± 0.535 b	990 ± 61 a	14.0 ± 1.82 a
Ctrl–PSB	866 ± 64.4 ab	5.73 ± 1.38 ab	1028 ± 58.5 a	14.5 ± 1.68 a
TSP	944 ± 58 ab	5.94 ± 0.631 ab	1005 ± 40.7 a	14.3 ± 0.590 a
TSP–PSB	879 ± 105 ab	5.36 ± 0.801 ab	1090 ± 38.7 a	15.7 ± 0.597 a
nHAP$_{300}$	849 ± 47.4 b	5.37 ± 0.431 ab	1014 ± 54.9 a	14.8 ± 1.03 a
nHAP$_{300}$–PSB	863 ± 50.7 ab	6.04 ± 0.415 ab	1020 ± 68.8 a	14.3 ± 1.26 a
nHAP$_{700}$	899 ± 91.8 ab	6.82 ± 0.951 ab	1032 ± 44.4 a	15.3 ± 0.635 a
nHAP$_{700}$–PSB	941 ± 51.2 ab	7.06 ± 0.18 a	1084 ± 56.5 a	15.9 ± 1.22 a
ANOVA p	*0.0236 **	*0.0091 ***	*0.0571 ns*	*0.1651 ns*

respectively. Also, in the case of P concentration in the plant aerial tissues, the lowest P value was observed in Ctrl (990 mg kg^{-1}), while the highest was in nHAP-PSB (1084 mg kg^{-1}). Although the ANOVA did not highlight a significant effect of the treatments, the value of $p = 0.0571$ indicated a clear trend (Table 2).

The concentrations of Ca, Fe, K, Mg, Mn, and S in roots and aerial tissues of *H. vulgare* are respectively reported in Tables 3–4.

We examined together K and Mn concentrations, since the two-way ANOVA highlighted the interaction between the main factors FERT and PSB. However, the actual significance of the interaction was the opposite. In the case of K concentration, the statistically significant interaction ($F(7,32) = 7.3351$, $p = 0.0007$***) was due to the more substantial accumulation of K in the root tissues of the control plants (6.54 g kg^{-1}) compared to the fertilized ones which had a K concentration in the roots between 5.11 and 4.16 g kg^{-1} (Table 3). In the case of Mn, the interaction FERT X PSB ($F(7,32) = 6.1705$, $p = 0.0020$**) was likely due to the increase in Mn accumulation in the root tissues of barley plants in response to fertilization with nHAP. The effect of PSB treatment on Mn accumulation in root tissues was not statistically significant. Averaging the data relating to the PSB treatment, TSP corresponds to a concentration of Mn in the roots of 103 mg kg^{-1}, while in the $nHAP_{300}$ and $nHAP_{700}$ plants it was 145 and 186 mg kg^{-1} of Mn, respectively. From the outcome of the Tukey test, it is evident that fertilization with nHAP promotes a significant increase in the concentration of Mn in the roots, which goes from 103 mg kg^{-1} (TSP) to 144 mg kg^{-1} and 186 mg kg^{-1}, respectively, for $nHAP_{300}$ and $nHAP_{700}$ (Table 3).

Data regarding the concentrations of the secondary macronutrients Ca and Mg in the root tissues provided similar indications. The 1-factor ANOVA revealed a significant effect of treatments on the accumulation of Ca ($F(7,32) = 2.5637$, $p = 0.0324$*) and Mg (($F(7,32) = 2.6258$, $p = 0.0291$*) in root tissues of *H. vulgare*. For both elements, the highest concentrations were observed in plants treated with nHAP (Table 3). In the case of Fe concentration, although the highest values were observed in the roots of plants grown in the presence of $nHAP_{300}$ and $nHAP_{700}$, due to an elevated variability in the data among the same species, the ANOVA did not detect statistically significant differences between the fertilizer treatments (Table 3).

Concerning S, although the 2-ways ANOVA did not reveal the statistical significance of the interaction between the main factors, it highlighted a highly significant effect of the PSB factor ($F(1,32) = 18.6192$, $p = 0.0001$***). The average values of S concentration in the roots were 1.51 g kg^{-1} in roots inoculated with *P. alloputida* and 1.09 g kg^{-1} in the absence of PSB inoculation. The subsequent data analysis through the 1-way ANOVA and the post-hoc test indicated an evident influence of the treatments on the root uptake of S (Table 3). In particular, it was observed that: (i) the concentration of S progressively increases according to the order Ctrl < TSP < $nHAP_{300}$ < $nHAP_{700}$, (ii) regardless of the type of fertilization, inoculation with PSB determines an increase in the radical concentration of S. From a quantitative point of view, compared to the absence of bacterial inoculation, the increase is 50.5 % in Ctrl (1.41 g kg^{-1}), 39 % for TSP (1.52 g kg^{-1}), 40.3 % for $nHAP_{300}$ (1.58 g kg^{-1}) and finally 25.4 % for $nHAP_{700}$ (1.55 g kg^{-1}) (Table 3).

Finally, it was found that fertilizer treatments did not have a statistically significant effect on the accumulation of Ca, Fe, Mg, and Mn in the aerial tissues of *H. vulgare*. However, it did affect the accumulation of K and S (Table 4).

A statistically significant different K concentration was detected in the plant shoots' treatment ($F(7,32) = 2.4402$, $p = 0.0401$*). The detected values of K concentration in plant shoots were quite narrow, ranging from 23.4 to 26.9 g kg^{-1}. The $nHAP_{700}$ plants had lower K concentration values than those observed in the Ctrl plants. However, the highest concentrations were observed in the Ctrl plants, which is consistent with the K root concentration data (Table 4).

The concentration of S in the aerial tissues followed the same trend observed in the roots, although with slightly lower values. ANOVA showed a statistically significant effect of the treatments ($F(7,32) = 4.8095$, $p = 0.0000$***). The positive difference between the non-PSB and PSB treatments is statistically significant for Ctrl (+9.57 %), TSP (+12.2 %), and $nHAP_{700}$ (+8.93 %) but not for $nHAP_{300}$ (+6.48 %) (Table 4).

4. Discussion

Phosphorus is a vital macronutrient for crop growth. However, P nutrition management remains one of the most significant challenges in global agriculture. This is because the phosphate rocks used in P fertilizer production are a non-renewable resource which has been depleted in recent years. Moreover, overusing P fertilizers can harm the environment by causing surface water eutrophication (Johnston and Poulton, 2019). To ensure sustainable agriculture, it is imperative to improve the P use efficiency by crops. Much research has been conducted to find better ways to apply fertilizers. Two types of fertilizers have been created: (i) "controlled release fertilizers" that have the nutrient enclosed in organic or inorganic material, which regulates the nutrient's release, and (ii) "slow-release fertilizers" that release nutrients at a slower rate compared to soluble fertilizers and the release rate is solely dependent on the soil conditions (Rajan et al., 2021).

Nanoscale fertilizers are set to transform traditional crop fertilization techniques by significantly enhancing the macronutrient and micronutrient use efficiency, so they are part of precision agriculture (Kalia et al., 2020; Skrzypczak et al., 2022). Scientific research has demonstrated that improved nutrient use efficiency will reduce the amount of fertilizer required by crops. This same benefit can be extended to other nano agrochemicals. Studies conducted in laboratories, greenhouses and fields have shown that nanoscale fertilizers have a relatively high Technology Readiness Level (TRL) (Hofmann et al., 2020).

From the first evidence (Liu and Lal, 2014) up to the recent studies (Sigmon et al., 2023; Tang et al., 2023), the investigations into the fertilizer potential of nanoscale hydroxyapatite have largely focused on the synthetic form. However, since wastes and residues from agriculture and food industries are a valuable source for manufacturing low-cost, renewable, bio-based products (Nath et al., 2023), this work considered the use of two forms of biogenic nano-hydroxyapatite supplied to

Table 3
Element concentration in root tissues of *H. vulgare*. Data are mean ± standard error (n=5). Different letters were used to indicate statistically significant differences between treatments with Tukey's post-hoc test ($p \leq 0.05$).

Treatment	Ca (g kg^{-1})	Fe (g kg^{-1})	K (g kg^{-1})	Mg (g kg^{-1})	Mn (mg kg^{-1})	S (g kg^{-1})
Ctrl	12.3 ± 1.21 b	1.90 ± 0.285 a	6.54 ± 0.191 a	5.20 ± 0.689 abc	84.7 ± 16 b	0.934 ± 0.07c
Ctrl–PSB	16.3 ± 1.33 ab	3.13 ± 0.681 a	4.58 ± 0.783 b	6.39 ± 0.741 abc	128 ± 47.9 b	1.41 ± 0.154 ab
TSP	14.0 ± 0.49 ab	3.10 ± 0.319 a	5.12 ± 0.191 b	4.24 ± 0.458 bc	121 ± 34.5 b	1.10 ± 0.132 bc
TSP–PSB	12.3 ± 0.74 b	2.33 ± 0.179 a	4.39 ± 0.562 b	3.11 ± 0.16c	85.6 ± 13.1 b	1.52 ± 0.207 a
$nHAP_{300}$	20.0 ± 3.48 ab	3.92 ± 1.04 a	4.30 ± 0.444 b	8.09 ± 1.91 abc	128 ± 24.8 b	1.12 ± 0.219 bc
$nHAP_{300}$–PSB	21.4 ± 3.80 ab	3.23 ± 0.279 a	4.70 ± 0.888 b	10.5 ± 1.51 a	161 ± 67 b	1.58 ± 0.205 a
$nHAP_{700}$	22.1 ± 3.42 ab	3.84 ± 0.469 a	4.77 ± 0.379 b	9.65 ± 1.43 ab	232 ± 98.4 a	1.23 ± 0.184 abc
$nHAP_{700}$–PSB	24.5 ± 2.95 a	3.99 ± 0.375 a	4.16 ± 0.664 b	10.4 ± 1.89 a	141 ± 31.3 ab	1.55 ± 0.289 a
ANOVA p	*0.0061* **	*0.0736 ns*	*0.0000* ***	*0.0005* ***	*0.0014* **	*0.0000* ***

Table 4
Element concentration in aerial tissues of *H. vulgare*. Data are mean ± standard error (n=5). Different letters were used to indicate statistically significant differences between treatments with Tukey's post-hoc test ($p \leq 0.05$).

Treatment	Ca (g kg^{-1})	Fe (mg kg^{-1})	K (g kg^{-1})	Mg (g kg^{-1})	Mn (mg kg^{-1})	S (g kg^{-1})
Ctrl	5.95 ± 0.424 a	127 ± 48.5 a	25.9 ± 0.983 a	3.96 ± 0.34 a	44.0 ± 4.74 a	1.18 ± 0.119 b
Ctrl–PSB	6.09 ± 0.196 a	129 ± 54 a	26.1 ± 0.572 a	4.04 ± 0.14 a	45.7 ± 3.47 a	1.29 ± 0.065 ab
TSP	5.73 ± 0.205 a	146 ± 56.8 a	24.4 ± 0.893 b	3.86 ± 0.246 a	43.3 ± 1.21 a	1.19 ± 0.074 b
TSP–PSB	5.84 ± 0.305 a	144 ± 54.8 a	25.3 ± 1.02 ab	3.91 ± 0.152 a	43.2 ± 2.05 a	1.34 ± 0.035 ab
$nHAP_{300}$	5.81 ± 0.292 a	127 ± 58.1 a	25.4 ± 0.390 ab	4.06 ± 0.26 a	43.9 ± 3.99 a	1.26 ± 0.10 ab
$nHAP_{300}$–PSB	5.99 ± 0.284 a	178 ± 39.2 a	25.1 ± 0.656 ab	3.99 ± 0.326 a	47.5 ± 3.36 a	1.35 ± 0.112 aa
$nHAP_{700}$	5.92 ± 0.198 a	156 ± 72.1 a	24.9 ± 1.16 ab	4.17 ± 0.154 a	46.6 ± 5.05 a	1.31 ± 0.055 ab
$nHAP_{700}$–PSB	5.63 ± 0.178 a	132 ± 18.1 a	24.6 ± 0.838 b	4.22 ± 0.263 a	44.5 ± 2.87 a	1.43 ± 0.074 a
ANOVA p	*0.1983 ns*	*0.8109 ns*	*0.0401 **	*0.2863 ns*	*0.4643 ns*	*0.0009 ****

barley plants in combination with a PSB.

The initial step of this study involved synthesizing a material capable of efficiently recovering P from waste. The developed nanoparticles exhibit a P content of 128 ± 2.77 g mg^{-1} for $nHAP_{300}$ and 196 ± 2.31 g mg^{-1} for $nHAP_{700}$, respectively. Notably, the P content of $nHAP_{700}$ surpasses that of commercial TSP, which typically contains less than 20 % phosphorus. The second step was to assess the toxicity of these new powders on seeds. In fact, one possibility could be that $nHAP_{300}$ is harmful to seeds and seedlings due to the presence of aromatic compounds in unburnt organic matter, as biochar is (Bai et al., 2022). The data collected from the germination trial confirm that nHAPs, supplied in various and high concentrations, did not lead to any decreases in the germination rate of *H. vulgare*. Similar results were also obtained in other studies carried out under different conditions and on species such as *Cicer arietinum* (Bala et al., 2014.), *Cucumis sativus* (Liu et al., 2015), *Cyamopsis tetragonoloba* (Shylaja et al., 2022), *Oryza sativa* (Wu et al., 2023), and *Solanum lycopersicum* (Marchiol et al., 2019). The elemental analysis performed on the samples did not detect any toxic elements (i.e., Pb, Cd or other trace metals) that could affect seeds and their germination (Fig. 4 A). The stimulating effect on the early development phases of the root system found in seedlings treated in pre-germination with $nHAP_{300}$ is interesting and promising (Fig. 4 C). The root-stimulating effect observed is probably due to the presence of other macro and microelements contained in the structure of nHAP and released by it, giving benefit to the seed germination. This aspect has to be investigated more in detail; indeed, the solubilization and the release of the elements should be studied, as it may depend on the sample, as well as the conditions. As stated above, $nHAP_{300}$ has a much higher content of C and N in comparison to $nHAP_{700}$; it is reasonable to think that, during imbibition, both these elements were transferred to the seeds. This could explain the higher values in the root length observed for *H. vulgare*. The use of nanostructure to deliver more nutrients is one of the objectives of nano-enabled agriculture; these results, therefore, are in line with this.

In the third step, the aim was to test these materials on plants. During the experimental design drafting, we considered some reviews that confirmed the promising potential of nano-enabled agriculture (NEA), but also highlighted some weaknesses in the setup of several trials (Kah et al., 2019; Santos et al., 2022). The plant growth trial had two sub-objectives. Firstly, the comparison of the effects of conventional phosphate fertilization (TSP) with the nanoscale P source. Secondly, the comparison of the fertilizing performance of two forms of nHAP synthesized using a thermal treatment with two different processing temperatures, resulting in one form with partially combusted organic components and one without. We also inoculated the "soil-plant system" with PSB to evaluate the influence of bacterial activity on the release of P for the benefit of the plants. All these aspects were closely linked to the nature and to the composition of the nHAP.

When studying a plant species, we can determine its health and response to stress by examining various biometric parameters. These include the plant's height, number of nodes and leaves, root system development, and architecture. Roots are the primary organs that absorb water and nutrients, so they play a vital role in P uptake from soil. When plants face low phosphorus availability, they typically adapt by changing their root physiology and morphology. In barley, for example, researchers have observed that phosphorus deficiency promotes an increase in the root-to-shoot ratio, as well as the formation of lateral roots and root hairs (Heydari et al., 2019; Lynch and Brown, 2008).

A recent hydroponic study elegantly examined the relationship between nHAP and the roots of P-deficient barley plants. The study provided the first evidence of the recovery of physiological status after treatment with nHAP. Additionally, the study explained how nHAP enters the root epidermis and moves via the apoplast, releasing P that is transported to the vascular system in the form of ionic PO_4^{3-}. This P is then translocated to the aerial plant tissues (Szameitat et al., 2021). In this study, barley plants were grown in an agricultural soil well-endowed with P; therefore, the increase in root weight does not respond to P-shortage. Indeed, the root weight in both Ctrl and TSP plants was rather much the same, whereas the plants responded to $nHAP_{300}$ and $nHAP_{700}$ by increasing the root biomass more than with TSP (Fig. 5).

As reported above, the effect found at the root system's level was not observed in the aerial biomass. Contrarily, literature reported a positive impact of nHAP on the development of aerial biomass in *Oryza sativa* (Pongpeera and Maensiri, 2023) and *Cyamopsis tetragonoloba* (Shylaja et al., 2022). By extending the experiment for the entire life cycle, it may be possible that the plants would have shown the effect of $nHAP_{300}$ and $enHAP_{700}$ on aerial biomass later. Indeed, more investigations should be performed to verify this.

Regarding the observations in this work on the non-significant effects of PSB, there are still gaps in our understanding of the mechanisms of action of the P mobilization process and the connection between PSB populations and the dynamics of the agroecosystem. Indeed, as reported in literature, many uncertainties remain regarding PBS implementation in open fields (Cheng et al., 2023). In this study, the statistical analysis did not identify any significant effect of the PSB factor on biometric variables. The variability of the data has hidden the statistical validation of the impact of the PSB factor, which is understood graphically. It is possible that by prolonging the experiment until the end of the plant's cycle, these effects could be observed.

The need to develop best management practices for fertilization is urgent to improve the sustainability of primary production. The environmental concerns and debates about the issue of "peak P" have increased efforts to maximize P use efficiency for high crop yield (Bindraban et al., 2020). The Olsen method is a widely accepted soil test used to determine soil P fertility in mildly acidic, neutral or alkaline soils (Battisti et al., 2022). Although more advanced tools are available to represent the complex dynamics of P in soil, Olsen P clearly showed the role of PSB (Wanke et al., 2023). In the relatively P-rich soil used in this experiment with barley, fertilization with TSP or nHAP had little influence on the available P fraction. The effect of PSB is decisive, especially when fertilization is carried out using $nHAP_{300}$. However, the fertilizing potential of nHAP is limited by the rate of P dissolution, requiring the development of strategies to overcome this issue. Recent

studies confirm that the dynamics of P release from nHAP are positively influenced by the presence of bacteria belonging to *Burkholderiaceae*, *Massilia*, *Pseudomonas*, *Sinomonas*, and *Streptomyces* (A. Santana et al., 2019; Quattrocelli et al., 2023; Li et al., 2023) genera. The observed effects shown by the nHAP-PSB complex are one of the most relevant findings of this experiment.

In addition to plant growth, the uptake and subsequent allocation of some nutritional elements in the root and aerial tissues of *H. vulgare* fertilized with $nHAP_{300}$ and $nHAP_{700}$ were considered. Some studies have shown that it is possible to produce nano-hydroxyapatite (nHAP) doped with macro- and micronutrients such as Fe^{2+}, Fe^{3+}, Mg^{2+}, Zn^{2+}, Cu^{2+}, K^{+}, Mo^{2+} and co-doping with Zn-Mg. Regarding the present study, as the nHAP materials are derived from bones, they already contain some of these elements in small concentrations (see Table 1); indeed, this represents a further advantage in the use of biogenic nHAP compared to synthetic ones.

In addition to interactions with PSB, various synthesis protocols have been studied to address this limit by varying process parameters such as temperature, pH and ions substitution. These parameters can improve control over the release of P, as substitution with specific ions can increase the solubility of some phosphate phases (Sakhno et al., 2022). This study confirmed the literature findings that the different elemental composition of the two forms of nHAP positively affected the assimilation and allocation of some nutrient elements in the plant tissues. This evidence was observed more prominently in the root tissues than in aboveground ones.

As mentioned previously, this study is preliminary, and it is possible that the effects of fertilizer treatments on the assimilation and distribution of elements in the root and aerial biomass, as well as in the composition of barley kernels, would be more pronounced. Furthermore, it has to be highlighted that these positive results were achieved using nHAP extracted from residues of the food industry. This implies a significant lower impact on the environment. This HAP, in fact, does not use any non-renewable resources for its production but, on the contrary, valorizes the P present in a waste material.

P concentration in chicken bones may vary slightly due to the origin of the animal and/or its age and development (Macavei et al., 2024); this could lead to nHAP with slightly different P concentrations. In all cases, however, P is still one of the main components. The scope of this work was to show as proof of concept that the bone residues of the food industry have potential to be used to produce sustainable fertilizers. For applications at larger and more industrial levels, it might be necessary to adjust the synthesis protocol, for instance including some steps prior to the thermal treatment, i.e., selection of the bones with higher P content or elemental analysis of bones.

A full Life Cycle Assessment (LCA) of nHAP production from chicken bones and their effectiveness as sustainable fertilizers is outside the scope of this work; some considerations, however, can still be made. Chicken is one of the most consumed meats in almost every country of the world, with annual consumption pro-capita higher than 40 kg for several countries and overall consumption of millions of tonnes worldwide (Helgi Library, 2023); moreover, chicken is not a seasonal product. These features make its residues available in large quantities and all year around. Indeed, there are costs and an environmental impact associated with nHAP extraction from bones. However, it must be noted that also in the production of standard fertilizers there are costs, and the processes have an impact on the environment. Therefore, to assess if these nHAP are more sustainable, a study should also include a comparison with the production of standard fertilizers. These elements surely play a key role in the economic viability and sustainability of nHAP derived from chicken bones.

5. Conclusions

This study demonstrates the effectiveness of two types of biogenic nano-hydroxyapatite (nHAP) synthesized using a top-down approach from waste materials, specifically chicken bones. The results are highly promising, revealing that these nHAP nanoparticles, characterized by high P content, are non-toxic and can promote root elongation during germination. Remarkably, these nHAPs perform comparably to, or even better than, traditional triple superphosphate (TSP) fertilizer, enhancing biomass and improving tissue elemental composition due to the natural presence of additional ions. Furthermore, the presence of *Pseudomonas alloputida* enhances phosphorus uptake and bioavailability in the soil.

This study highlights the fertilizing potential of nHAP extracted from food industry residues, emphasizing its beneficial composition and the role of phosphorus-solubilizing bacteria (PSB) in P mobilization. The findings suggest that biogenic nHAPs could be a sustainable alternative to conventional fertilizers, offering environmental and agricultural benefits by recycling waste materials. However, further research is needed to evaluate the full crop cycle implications of P nano-fertilization on yield quantity and grain quality. Additionally, the use of waste biological materials in sustainable agriculture aligns with the goals of EU Farm2Fork Strategy, promoting resource recovery and valorization.

CRediT authorship contribution statement

Guido Fellet: Writing – review & editing, Methodology, Investigation, Conceptualization. **Laura Pilotto:** Writing – original draft, Investigation, Formal analysis, Conceptualization. **Monica Yorlady Alzate Zuluaga:** Writing – review & editing, Methodology, Investigation. **Francesca Scalera:** Writing – review & editing, Methodology, Investigation. **Clara Piccirillo:** Writing – review & editing, Methodology, Investigation. **Luca Marchiol:** Writing – review & editing, Funding acquisition, Conceptualization. **Marcello Civilini:** Methodology. **Youry Pii:** Writing – review & editing, Methodology, Investigation. **Stefano Cesco:** Writing – review & editing, Methodology.

Declaration of Competing Interest

The authors declare that they have no known competing financial interests or personal relationships that could have appeared to influence the work reported in this paper.

Data Availability

Data will be made available on request.

Acknowledgements

This work was supported by Italian Ministry of University – Projects of Relevant Interest 2023–2025. PRIN2022-2022AAATEA – Circular economy and sustainable agriculture: Hydroxyapatite from Biowastes as Smart Nanofertilizer – Cleopatra. The authors also thank Sofia Tuzzi and Lorenzo Sinigaglia for their relevant contribution to the work and prof. Robert C. Pullar for the revision of the English language.

References

A. Santana, C., Piccirillo, C., A. Pereira, S.I., Pullar, R.C., Lima, S.M., L. Castro, P.M., 2019. Employment of phosphate solubilising bacteria on fish scales – turning food waste into an available phosphorus source. J. Env Chem. Eng. 7 (2019), 103403 https://doi.org/10.1016/j.jece.2019.103403.

Ahmed, M., Nigussie, A., Addisu, S., Belay, B., Sato, S., 2021. Valorization of animal bone into phosphorus biofertilizer: effects of animal species, thermal processing method, and production temperature on phosphorus availability. Soil Sci. Plant Nutr. 67 (2021), 471–481. https://doi.org/10.1080/00380768.2021.1945403.

Alao, B.O., Falowo, A.B., Chulayo, A., Muchenje, V., 2017. The potential of animal by-products in food systems: production, prospects and challenges. Sust 9 (2017), 1089. https://doi.org/10.3390/su9071089.

Bai, X., Zhang, S., Shao, J., Chen, Anwei, Jiang, J., Chen, Ang, Luo, S., 2022. Exploring the negative effects of biochars on the germination, growth, and antioxidant system of rice and corn (Engineering). J. Env Chem. 10 (2022), 107398. https://doi.org/10.1016/j.jece.2022.107398.

Baig, N., Kammakakam, I., Falath, W., 2021. Nanomaterials: a review of synthesis methods, properties, recent progress, and challenges. Mat. Adv. 2 (2021), 1821–1871. https://doi.org/10.1039/D0MA00807A.

Bala, N., Dey, A., Das, S., Basu, R., Nandy, P., 2014. Effect of Hydroxyapatite nanorod on chickpea (*Cicer arietinum*) plant growth and its possible use as nano-fertilizer. Iranian J. Plant Phys. 4 (2014), 1061–1069, 3.

Battisti, M., Moretti, B., Sacco, D., Grignani, C., Zavattaro, L., 2022. Soil Olsen P response to different phosphorus fertilization strategies in long-term experiments in NW Italy. Soil Use Manag 38 (2022), 549–563. https://doi.org/10.1111/sum.12701.

Bindraban, P.S., Dimkpa, C.O., Pandey, R., 2020. Exploring phosphorus fertilizers and fertilization strategies for improved human and environmental health. Biol. Fertil. Soils 56 (2020), 299–317. https://doi.org/10.1007/s00374-019-01430-2.

C. Teixeira, M.A., Piccirillo, C., Tobaldi, D.M., Pullar, R.C., Labrincha, J.A., Ferreira, M. O., L. Castro, P.M., E. Pintado, M.M., 2017. Effect of preparation and processing conditions on UV absorbing properties of hydroxyapatite-Fe_2O_3 sunscreen. Mat. Sci. Eng. C 71 (2017), 141–149. https://doi.org/10.1016/j.msec.2016.09.065.

Carmona, F.J., Guagliardi, A., Masciocchi, N., 2022. Nanosized calcium phosphates as novel macronutrient nano-fertilizers. Nanom 12 (2022), 2709. https://doi.org/10.3390/nano12152709.

Cestari, F., Agostinacchio, F., Galotta, A., Chemello, G., Motta, A., M. Sglavo, V., 2021. Nano-hydroxyapatite derived from biogenic and bioinspired calcium carbonates: synthesis and in vitro bioactivity. Nanom 11 (2021), 264. https://doi.org/10.3390/nano11020264.

Cheng, Y., Narayanan, M., Shi, X., Chen, X., Li, Z., Ma, Y., 2023. Phosphate-solubilizing bacteria: their agroecological function and optimistic application for enhancing agro-productivity. Sci. Tot Env 901 (2023), 166468. https://doi.org/10.1016/j.scitotenv.2023.166468.

Dou, L., Zhang, Y., Sun, H., 2018. Advances in synthesis and functional modification of nanohydroxyapatite. J. Nanom (2018), 3106214. https://doi.org/10.1155/2018/3106214.

Fellet, G., Pilotto, L., Marchiol, L., Braidot, E., 2021. Tools for nano-enabled agriculture: fertilizers based on calcium phosphate, silicon, and chitosan nanostructures. Agron 11 (2021), 1239. https://doi.org/10.3390/agronomy11061239.

Gervaso, F., Scalera, F., Kunjalukkal Padmanabhan, S., Sannino, A., Licciulli, A., 2012. High-performance hydroxyapatite scaffolds for bone tissue engineering applications. Int J. Appl. Ceram. Techn 9 (2012), 507–516. https://doi.org/10.1111/j.1744-7402.2011.02662.x.

Gunaratne, G.P., Kottegoda, N., Madusanka, N., Munaweera, I., Sandaruwan, C., Priyadarshana, W.M.G.I., Siriwardhana, A., Madhushanka, B. a D., Rathnayake, U. A., Karunaratne, V., 2016. Two new plant nutrient nanocomposites based on urea coated hydroxyapatite: efficacy and plant uptake. Ind. J. Agr. Sci. 86 (2016), 494–499. https://doi.org/10.56093/ijas.v86i4.57483.

Gunes, A., Taskın, M.B., Taskın, H., Akca, H., Kan, S., Babar, S.K., 2024. Investigation of the time-dependent presence and residual effects of nanohydroxyapatite and diammonium phosphate in a barley-barley-maize-maize cropping system. J. Plant Nutr. 47 (2024), 1513–1526. https://doi.org/10.1080/01904167.2024.2315970.

Helgi Library 2023. Poultry Meat Consumption Per Capita. https://www.helgilibrary.com/indicators/poultry-meat-consumption-per-capita (accessed 5.25.24).

Heydari, M.M., Brook, R.M., Jones, D.L., 2019. The role of phosphorus sources on root diameter, root length and root dry matter of barley (*Hordeum vulgare* L. J. Plant Nutr. 42 (2019), 1–15. https://doi.org/10.1080/01904167.2018.1509996.

Hofmann, T., Lowry, G.V., Ghoshal, S., Tufenkji, N., Brambilla, D., Dutcher, J.R., Gilbertson, L.M., Giraldo, J.P., Kinsella, J.M., Landry, M.P., Lovell, W., Naccache, R., Paret, M., Pedersen, J.A., Unrine, J.M., White, J.C., Wilkinson, K.J., 2020. Technology readiness and overcoming barriers to sustainably implement nanotechnology-enabled plant agriculture. Nat. Food 1 (2020), 416–425. https://doi.org/10.1038/s43016-020-0110-1.

Jia, X., Shi, N., Tang, W., Su, Z., Chen, H., Tang, Y., Sun, B., Zhao, L., 2022. Nano-hydroxyapatite increased soil quality and boosted beneficial soil microbes. Plant Nano Bio 1 (2022), 100002. https://doi.org/10.1016/j.plana.2022.100002.

Johnston, A.E., Poulton, P.R., 2019. Phosphorus in agriculture: a review of results from 175 years of Research at Rothamsted, UK. J. Env Qual. 48 (2019), 1133–1144. https://doi.org/10.2134/jeq2019.02.0078.

Kah, M., Tufenkji, N., White, J.C., 2019. Nano-enabled strategies to enhance crop nutrition and protection. Nat. Nanotechnol. 14 (2019), 532–540. https://doi.org/10.1038/s41565-019-0439-5.

Kalia, A., Sharma, S.P., Kaur, Harleen, Kaur, Harsimran, 2020. Chapter 5 - Novel nanocomposite-based controlled-release fertilizer and pesticide formulations: Prospects and challenges. In: Abd-Elsalam, K.A. (Ed.), Multifunctional Hybrid Nanomaterials for Sustainable Agri-Food and Ecosystems, Micro and Nano Technologies. Elsevier, pp. 99–134. https://doi.org/10.1016/B978-0-12-821354-4.00005-4.

Kottegoda, N., Sandaruwan, C., Priyadarshana, G., Siriwardhana, A., Rathnayake, U.A., Berugoda Arachchige, D.M., Kumarasinghe, A.R., Dahanayake, D., Karunaratne, V., Amaratunga, G.A.J., 2017. Urea-hydroxyapatite nanohybrids for slow release of nitrogen. ACS Nano 11 (2017), 1214–1221. https://doi.org/10.1021/acsnano.6b07781.

Li, H.-P., Han, Q.-Q., Liu, Q.-M., Gan, Y.-N., Rensing, C., Rivera, W.L., Zhao, Q., Zhang, J.-L., 2023. Roles of phosphate-solubilizing bacteria in mediating soil legacy phosphorus availability. Micro Res 272 (2023), 127375. https://doi.org/10.1016/j.micres.2023.127375.

Liu, R., Lal, R., 2014. Synthetic apatite nanoparticles as a phosphorus fertilizer for soybean (*Glycine max*). Sci. Rep. 4 (2014), 5686. https://doi.org/10.1038/srep05686.

Liu, W., Wang, S., Sun, H., Zuo, Q., Lai, Y., Hou, J., 2015. Impact of nanometer hydroxyapatite on seed germination and root border cell characteristics. RSC Adv. 5 (2015), 82726–82731. https://doi.org/10.1039/C5RA13187A.

Lowry, G.V., Avellan, A., Gilbertson, L.M., 2019. Opportunities and challenges for nanotechnology in the agri-tech revolution. Nat. Nanotechnol. 14 (2019), 517–522. https://doi.org/10.1038/s41565-019-0461-7.

Lynch, J.P., Brown, K.M., 2008. Root strategies for phosphorus acquisition. In: White, P. J., Hammond, J.P. (Eds.), The Ecophysiology of Plant-Phosphorus Interactions. Springer Netherlands, Dordrecht, pp. 83–116. https://doi.org/10.1007/978-1-4020-8435-5_5.

Macavei, M.G., Gheorghe, V.-C., Ionescu, G., Volceanov, A., Pătrașcu, R., Mărculescu, C., Magdziarz, A., 2024. Thermochemical conversion of animal-derived waste: a mini-review with a focus on chicken bone waste. Processes 12 (2024), 358. https://doi.org/10.3390/pr12020358.

Madusanka, N., Sandaruwan, C., Kottegoda, N., Sirisena, D., Munaweera, I., De Alwis, A., Karunaratne, V., Amaratunga, G.A.J., 2017. Urea–hydroxyapatite-montmorillonite nanohybrid composites as slow release nitrogen compositions. Appl. Clay Sci. 150 (2017), 303–308. https://doi.org/10.1016/j.clay.2017.09.039.

Maghsoodi, M.R., Ghodszad, L., Asgari Lajayer, B., 2020. Dilemma of hydroxyapatite nanoparticles as phosphorus fertilizer: potentials, challenges and effects on plants. Env Techn Inn. 19 (2020), 100869 https://doi.org/10.1016/j.eti.2020.100869.

Marchiol, L., Filippi, A., Adamiano, A., Degli Esposti, L., Iafisco, M., Mattiello, A., Petrussa, E., Braidot, E., 2019. Influence of hydroxyapatite nanoparticles on germination and plant metabolism of tomato (*Solanum lycopersicum* L.): preliminary evidence. Agron 9 (2019), 161. https://doi.org/10.3390/agronomy9040161.

Maschmeyer, T., Luque, R., Selva, M., 2020. Upgrading of marine (fish and crustaceans) biowaste for high added-value molecules and bio(nano)-materials. Chem. Soc. Rev. 49 (2020), 4527–4563. https://doi.org/10.1039/C9CS00653B.

Monroy Miguel, R., Carrillo González, R., Rios Leal, E., González-Chávez, Ma. del C.A., 2020. Screening bacterial phosphate solubilization with bulk-tricalcium phosphate and hydroxyapatite nanoparticles. Antonie Van. Leeuwenhoek 113 (2020), 1033–1047. https://doi.org/10.1007/s10482-020-01409-2.

Montalvo, D., McLaughlin, M.J., Degryse, F., 2015. Efficacy of hydroxyapatite nanoparticles as phosphorus fertilizer in andisols and oxisols. Soil Sci. Soc. Am. J. 79 (2015), 551–558. https://doi.org/10.2136/sssaj2014.09.0373.

Nath, P.C., Ojha, A., Debnath, S., Sharma, M., Sridhar, K., Nayak, P.K., Inbaraj, B.S., 2023. Biogeneration of valuable nanomaterials from agro-wastes: a comprehensive review. Agron 13 (2023), 561. https://doi.org/10.3390/agronomy13020561.

Phan, K.S., Nguyen, H.T., Le, T.T.H., Vu, T.T.T., Do, H.D., Vuong, T.K.O., Nguyen, H.N., Tran, C.H., Ngo, T.T.H., Ha, P.T., 2019. Fabrication and activity evaluation on Asparagus officinalis of hydroxyapatite based multimicronutrient nano systems. Adv. Nat. Sci. Nanosci. Nanotechnol. 10 (2019), 025011 https://doi.org/10.1088/2043-6254/ab21cc.

Piccirillo, C., Adamiano, A., Tobaldi, D.M., Montalti, M., Manzi, J., Castro, P.M.L., Panseri, S., Montesi, M., Sprio, S., Tampieri, A., Iafisco, M., 2017. Luminescent calcium phosphate bioceramics doped with europium derived from fish industry byproducts. JACerS 100 (2017), 3402–3414. https://doi.org/10.1111/jace.14884.

Pohshna, C., Mailapalli, D.R., 2023. Characterization and testing of nanohydroxyapatite synthesized from eggshells as a phosphorus source for rice crops. J. Soil Sci. Plant Nutr. 23 (2023), 4491–4504. https://doi.org/10.1007/s42729-023-01366-5.

Pongpeera, S., Maensiri, D., 2023. Application of hydroxyapatite nanoparticles as fertilizer improved yield quality of rice (*Oryza sativa* L, 5 Chiang Mai J. Sci. 50 (2023), 1–12. https://doi.org/10.12982/CMJS.2023.053.

Pradhan, S., Durgam, M., Mailapalli, D.R., 2021. Urea loaded hydroxyapatite nanocarrier for efficient delivery of plant nutrients in rice. Arch. Agron. Soil Sci. 67 (2021), 371–382. https://doi.org/10.1080/03650340.2020.1732940.

Priyam, A., Das, R.K., Schultz, A., Singh, P.P., 2019. A new method for biological synthesis of agriculturally relevant nanohydroxyapatite with elucidated effects on soil bacteria. Sci. Rep. 9 (2019), 15083 https://doi.org/10.1038/s41598-019-51514-0.

Priyam, A., Yadav, N., Reddy, P.M., Afonso, L.O.B., Schultz, A.G., Singh, P.P., 2022b. Fertilizing benefits of biogenic phosphorous nanonutrients on *Solanum lycopersicum* in soils with variable pH. Heliyon 8 (2022), e09144. https://doi.org/10.1016/j.heliyon.2022.e09144.

Priyam, A., Yadav, N., Reddy, P.M., Afonso, L.O.B., Schultz, A.G., Singh, P.P., 2022a. Uptake and benefits of biogenic phosphorus nanomaterials applied via fertigation to Japonica Rice (Taipei 309) in low- and high-calcareous soil conditions. ACS Agric. Sci. Technol. 2 (2022), 462–476. https://doi.org/10.1021/acsagscitech.1c00244.

Quattrocelli, P., Pellegrino, E., Piccirillo, C., Pullar, R.C., Ercoli, L., 2023. Designing of novel hydroxyapatite nanoparticles from fish by-products to be coupled with highly efficient phosphate solubilising bacteria (No. EGU23-7293). Presented at the EGU23, Copernicus Meetings (2023). https://doi.org/10.5194/egusphere-egu23-7293.

Raguraj, S., Wijayathunga, W.M.S., Gunaratne, G.P., Amali, R.K.A., Priyadarshana, G., Sandaruwan, C., Karunaratne, V., Hettiarachchi, L.S.K., Kottegoda, N., 2020. Urea–hydroxyapatite nanohybrid as an efficient nutrient source in *Camellia sinensis* (L.) Kuntze (tea). J. Plant Nutr. 43 (2020), 2383–2394. https://doi.org/10.1080/01904167.2020.1771576.

Rajan, M., Shahena, S., Chandran, V., Mathew, L., 2021. Chapter 3 - Controlled release of fertilizers—concept, reality, and mechanism. In: Lewu, F.B., Volova, T., Thomas, S., K.r., R. (Eds.), Controlled Release Fertilizers for Sustainable Agriculture. Academic Press, pp. 41–56. https://doi.org/10.1016/B978-0-12-819555-0.00003-0.

Sakhno, Y., Ma, C., Borgatta, J., Jin, Y., White, J.C., Jaisi, D.P., 2022. Role of cation substitution and synthesis condition in a calcium phosphate-based novel nanofertilizer on lettuce (*Lactuca sativa*) Yield. ACS Sustain. Chem. Eng. 10 (2022), 15414–15422. https://doi.org/10.1021/acssuschemeng.2c04451.

Santos, E., Montanha, G.S., Gomes, M.H.F., Duran, N.M., Corrêa, C.G., Romeu, S.L.Z., Pereira, A.E.S., Oliveira, J.L., Almeida, E., Pérez-de-Luque, A., Ghoshal, S., Santaella, C., Lima, R., de, Fraceto, L.F., Carvalho, H.W.P., 2022. Are nanomaterials leading to more efficient agriculture? Outputs from 2009 to 2022 research metadata analysis. Environ. Sci. Nano 9 (2022), 3711–3724. https://doi.org/10.1039/D1EN01078F.

Scalera, F., Gervaso, F., Sanosh, K.P., Sannino, A., Licciulli, A., 2013. Influence of the calcination temperature on morphological and mechanical properties of highly porous hydroxyapatite scaffolds. Ceram. Int. 39 (2013), 4839–4846. https://doi.org/10.1016/j.ceramint.2012.11.076.

Shylaja, S., Prashanthi, Y., Nageswara Rao, T., 2022. Synthesis and evaluating the effects of nano hydroxyapatite on germination, growth and yield of cluster beans. Materials Today: Proceedings, International Conference on Advanced Materials for Innovation and Sustainability (2022). 64, 917–921. https://doi.org/10.1016/j.matpr.2022.06.054.

Sigmon, L.R., Vaidya, S.R., Thrasher, C., Mahad, S., Dimkpa, C.O., Elmer, W., White, J.C., Fairbrother, D.H., 2023. . Role of phosphorus type and biodegradable polymer on phosphorus fate and efficacy in a plant–soil system. J. Agric. Food Chem. 71 (2023), 16493–16503. https://doi.org/10.1021/acs.jafc.3c04735.

Singh, H., Sharma, A., Bhardwaj, S.K., Arya, S.K., Bhardwaj, N., Khatri, M., 2021. Recent advances in the applications of nano-agrochemicals for sustainable agricultural development. Environ. Sci.: Process. Impacts 23 (2021), 213–239. https://doi.org/10.1039/D0EM00404A.

Skrzypczak, D., Mikula, K., Izydorczyk, G., Taf, R., Gersz, A., Witek-Krowiak, A., Chojnacka, K., 2022. Chapter 4 - Smart fertilizers—toward implementation in practice. In: Chojnacka, K., Saeid, A. (Eds.), Smart Agrochemicals for Sustainable Agriculture. Academic Press, pp. 81–102. https://doi.org/10.1016/B978-0-12-817036-6.00010-8.

Subbaiya, R., Priyanka, M., Selvam, M., 2012. Formulation of green nano-fertilizer to enhance the plant growth through slow and sustained release of nitrogen. J. Pharm. Res. 5 (2012), 5178–5183.

Szameitat, A.E., Sharma, A., Minutello, F., Pinna, A., Er-Rafik, M., Hansen, T.H., Persson, D.P., Andersen, B., Husted, S., 2021. Unravelling the interactions between nano-hydroxyapatite and the roots of phosphorus deficient barley plants. Environ. Sci. Nano 8, 444–459. https://doi.org/10.1039/D0EN00974A.

Tang, S., Liang, J., Li, O., Shao, N., Jin, Y., Ni, J., Fei, X., Li, Z., 2023. Morphology-tailored hydroxyapatite nanocarrier for rhizosphere-targeted phosphorus delivery. Small 19 (2023), 2206954. https://doi.org/10.1002/smll.202206954.

Tiecher, T., Fontoura, S.M.V., Ambrosini, V.G., Araújo, E.A., Alves, L.A., Bayer, C., Gatiboni, L.C., 2023. Soil phosphorus forms and fertilizer use efficiency are affected by tillage and soil acidity management. Geoderma 435 (2023), 116495. https://doi.org/10.1016/j.geoderma.2023.116495.

US EPA, 1996a. Method 3052: Microwave assisted acid digestion of siliceous and organically based matrices. In: Test methods for evaluating solid waste, 3rd ed. Washington, DC: USEPA.

US EPA, 1996b. Ecological Effects Test Guidelines. OPPTS 850.4200. Seed Germination/Root Elongation Toxicity Test. US Environmental Protection Agency.

Wanke, D.J., Heichel, J., Zikeli, S., Müller, T., Hartmann, T.E., 2023. Comparison of soil phosphorus extraction methods regarding their suitability for organic farming systems. J. Plant NutrSoil Sci. 186 (2023), 599–608. https://doi.org/10.1002/jpln.202300129.

Wu, H., Jiang, X., Tong, J., Wang, J., Shi, J., 2023. Effects of Fe3O4 nanoparticles and nano hydroxyapatite on Pb and Cd stressed rice (*Oryza sativa* L.) seedling. Chemosphere 329 (2023), 138686 https://doi.org/10.1016/j.chemosphere (2023).138686.

Xin, X., Judy, J.D., Sumerlin, B.B., He, Z., 2020. Nano-enabled agriculture: from nanoparticles to smart nanodelivery systems. Environ. Chem. 17 (2020), 413–425. https://doi.org/10.1071/EN19254.

Xiong, L., Wang, P., Hunter, M.N., Kopittke, P.M., 2018. Bioavailability and movement of hydroxyapatite nanoparticles (HA-NPs) applied as a phosphorus fertiliser in soils. Environ. Sci.: Nano 5 (2018), 2888–2898. https://doi.org/10.1039/C8EN00751A.

Yoon, H.Y., Lee, J.G., Esposti, L.D., Iafisco, M., Kim, P.J., Shin, S.G., Jeon, J.-R., Adamiano, A., 2020. Synergistic release of crop nutrients and stimulants from hydroxyapatite nanoparticles functionalized with humic substances: toward a multifunctional nanofertilizer. ACS Omega 5 (2020), 6598–6610. https://doi.org/10.1021/acsomega.9b04354.

Yu, X., Keitel, C., Dijkstra, F.A., 2021. Global analysis of phosphorus fertilizer use efficiency in cereal crops. Glob. Food Secur. 29 (2021), 100545 https://doi.org/10.1016/j.gfs.2021.100545.